第 35 卷第 11 期 无 机 化 学 学 报 Vol.35 No.11
2019 年 11 月 CHINESE JOURNAL OF INORGANIC CHEMISTRY 2108-2116

锆簇基纳米分子胶囊的合成、晶体结构和荧光性质

陶艳丽[1] 陈维超*,[1] 王新龙[1] 苏忠民*,[1,2]
([1]东北师范大学化学学院,长春 130024)
([2]长春理工大学,长春 130024)

摘要:选取 4,4′-联苯二甲酸(4,4′-H_2BPDC)和 2,6-萘二甲酸(2,6-H_2NDC)分别与二氯二茂锆(Cp_2ZrCl_2)反应制备了 2 例结构新颖的锆基纳米分子胶囊$[Cp_3Zr_3(\mu_3\text{-}O)(\mu_2\text{-}OH)_3]_2(BPDC)_3Cl_2\cdot H_2O$ (**Zr-MC-1**)和$[Cp_3Zr_3(\mu_3\text{-}O)(\mu_2\text{-}OH)_3]_2(NDC)_3Cl_2\cdot 3H_2O$ (**Zr-MC-2**)。这 2 个分子胶囊均由 3 个线性羧基配体桥联 2 个三核茂锆建筑单元构成。利用单晶 X 射线衍射、粉末 X 射线衍射、元素分析、红外光谱、热重分析和氮气吸附–脱附等手段对化合物进行了表征。此外,荧光光谱分析表明 **Zr-MC-1** 和 **Zr-MC-2** 分别为深蓝光和蓝光发射材料,其最大发射波长分别为 404 和 456 nm。

关键词:分子胶囊;晶体结构;羧酸配体;荧光光谱
中图分类号:O614.41+2 **文献标识码**:A **文章编号**:1001-4861(2019)11-2108-09
DOI:10.11862/CJIC.2019.224

Synthesis, Crystal Structures and Fluorescence Properties of Two Nanosized Zr-Based Molecular Capsules

TAO Yan-Li[1] CHEN Wei-Chao*,[1] WANG Xin-Long[1] SU Zhong-Min*,[1,2]
([1]*Northeast Normal University, Changchun* 130024, *China*)
([2]*Changchun University of Science and Technology, Changchun* 130024, *China*)

Abstract: Two nanosized zirconium-based molecular capsules (Zr-MCs), namely $[Cp_3Zr_3(\mu_3\text{-}O)(\mu_2\text{-}OH)_3]_2(BPDC)_3Cl_2\cdot H_2O$ (**Zr-MC-1**) and $[Cp_3Zr_3(\mu_3\text{-}O)(\mu_2\text{-}OH)_3]_2(NDC)_3Cl_2\cdot 3H_2O$ (**Zr-MC-2**), have been synthesized by reacting zirconocenedichloride (Cp_2ZrCl_2) with 4,4′-biphenyldicarboxylic acid (4,4′-H_2BPDC) and 2,6-naphthalenedicarboxylic acid (2,6-H_2NDC), respectively, which are constructed by two trinuclear zirconocene building blocks and three linear carboxylate ligands. They were characterized by single-crystal X-ray diffraction, powder X-ray diffraction, elemental analysis, IR spectroscopy, thermogravimetric analysis and N_2 adsorption-desorption tests. In addition, the fluorescence spectra indicate that **Zr-MC-1** and **Zr-MC-2** are deep-blue and blue emitting materials with emission peaks at 404 and 456 nm, respectively. CCDC: 939840, **Zr-MC-1**; 939841, **Zr-MC-2**.

Keywords: molecular capsule; crystal structure; carboxylate ligand; fluorescence spectroscopy

0 Introduction

Metal-organic molecular capsules (MCs) remains discrete inorganic-organic molecular complexes that are built by the self-assembly of metal ions/clusters and organic linkers[1-3]. It has attracted extensively wide investigations as a result of its fascinating structures with adjustable inner cavities and potential

收稿日期:2019-07-29。收修改稿日期:2019-09-09。
国家自然科学基金(No.21801038,21471027,21671034),吉林省教育厅(No.JJKH20190271KJ),中国博士后基金资助项目(No.2018M630312, 2019T120227)和中央高校基本科研专项资金(No.2412018QD003)资助。
*通信联系人。E-mail:chenwc061@nenu.edu.cn,zmsu@nenu.edu.cn;会员登记号:S06N5404M1606(陈维超),S06N6890P1004(苏忠民)。

applications, such as gas storage-separation[4-6], magnetism[7-10], drug delivery[11-12], catalysis[4,13] together with guest molecule accommodating and release[13-14]. As is known to all, the reported secondary building units (SBUs) during the preparation of MCs mainly focuse on early transition metal centers, and the reversible property of such coordination bonds may bring poor water stability as well as limited applications in most research area of MCs.

Recently, Zr-based metal-organic frameworks featuring high stability in both acid and alkaline aqueous solutions owing to the quite strong Zr-O bonds (chemical bond energy: 776 kJ·mol^{-1}) have gained extensive interests[15]. Inspired by this aspect, in 2013, Yuan and co-workers has developed a facile strategy to access a family of Zr-based metal-organic polyhedra (MOPs) by reaction of bis(cyclopentadienyl)zirconium dichloride (Cp_2ZrCl_2, Cp =η^5-C_5H_5) with carboxyl ligands[16]. Such zirconocene precursor could be easily hydrolyzed in presence of water and carboxylate acid to achieve a trinuclear ligand-bridged Zr-cation moiety, namely $Cp_3Zr_3(\mu_3\text{-}O)(\mu_2\text{-}OH)_3$, which acts as 3-connected SBUs for the construction of various water-stable coordination polyhedra. Those MOPs show potential applications in catalysis[17], proton conductivity[18] and gas storage-separation[19], *etc*. So far, only several Zr-based MOPs have been discovered, and the rational design and synthesis of more Zr-based MOPs with specific architecture and functionality still possess a considerable challenge[15-23].

Taking into account the above backgrounds, we herein present the synthesis and crystal structures of two Zr-MCs constructed from trinuclear $Cp_3Zr_3(\mu_3\text{-}O)(\mu_2\text{-}OH)_3$ SBUs and linear dicarboxylate ligands. They were fully characterized by multiple analysis techniques and their photoluminescent properties were also described.

1 Experimental

1.1 Materials and physical measurements

All chemical reagents were derived from commerce and used directly without purification. PXRD patterns were measured from 5° to 50° through a Siemens D5005 diffractometer at 40 kV, 30 mA for Cu $K\alpha$ (λ=0.154 18 nm). Thermogravimetric analysis (TGA) of the crystal samples was tested using a PerkinElmer TG-7 analyzer by heating from 25 to 800 ℃ (10 ℃·min^{-1}) under a dry nitrogen environment. Elemental analyses (C, H, N) were performed on a PerkinElmer 2400 CHN Elemental analyzer. The FT-IR spectra were measured from 4 000 to 400 cm^{-1} using KBr pellets with an Alpha Centauri FT/IR spectrophotometer. N_2 gas adsorption-desorption and porosimetry were performed on ASIQM0G002-3. The solid-state photoluminescence (FL) spectra of both crystals and organic ligands were performed at room temperature using F-7000 FL spectrophotometer. A transient spectrofluorimeter (Edinburgh FLSP920) was used to test the excited-state lifetimes (τ) of the two compounds in solid state.

1.2 Preparations of Zr-MC-1 and Zr-MC-2

Zr-MC-1 was synthesized by reacting 4,4′-H_2BPDC (0.02 g, 0.08 mmol) and zirconocenedichloride (Cp_2ZrCl_2) (0.03 g, 0.1 mmol) in *N*,*N*-dimethylformamide (DMF, 1.0 mL), CH_3OH (1.0 mL) and water (5 drops) at 80 ℃ for 18 hours. After slowly cooling to room temperature, colorless crystals were obtained, washed with DMF and dried in air. Yield: 88% based on 4,4′-H_2BPDC. Elemental analysis Calcd. for $C_{72}H_{62}O_{20}Zr_6Cl$(%): C 47.33, H 3.29; Found(%): C 47.23, H 3.30. IR (KBr, cm^{-1}): 3 420 (m), 1 654 (m), 1 608 (m), 1 574 (s), 1 524 (s), 1 415 (s), 1 180 (w), 1 097 (w), 1 013 (m), 808 (w), 766 (w), 695 (w), 674 (m), 603 (m), 536 (m), 447 (s).

Zr-MC-2 was prepared by reacting 2,6-H_2NDC (0.02 g, 0.08 mmol) and zirconocenedichloride (Cp_2ZrCl_2) (0.03 g, 0.1 mmol) in *N*,*N*-dimethylformamide (DMF, 1.0 mL), CH_3OH (1.0 mL) and water (5 drops) at 80 ℃ for 12 hours. Colorless crystals were isolated (washed with DMF) when the oven was gradually cooled to room temperature. Yield: 90% based on 2,6-H_2NDC. Elemental analysis Calcd. for $C_{66}H_{60}O_{23}Zr_6Cl_2$ (%): C 43.11, H 3.27; Found (%): C 43.31, H 3.20. IR (KBr, cm^{-1}): 3 198 (m), 2 930 (w), 1 657 (s), 1 599 (s), 1 553 (s), 1 494 (w), 1 419 (s), 1 365 (s), 1 247 (w), 1 197 (w), 1 092 (w), 1 017 (w), 921 (w), 812 (m), 787 (m),

770 (w), 658 (w), 607 (m), 490 (m).

1.3 Single-crystal X-ray crystallography

Single-crystal X-ray crystallography data were collected at 298 K on Bruker D8 VENTURE with micro-focus Cu $K\alpha$ radiation (λ=0.154 178 nm). Absorption corrections were achieved by a multi-scan technique. The structures were solved by direct methods, and further refinement of the structures was performed by using full-matrix least squares techniques with SHELXL-2014 program[24]. Hydrogen atoms were fixed geometrically at calculated positions and allowed to ride on the parent non-H atoms. All the non-H atoms were refined ansiotropically during the refinement. Additionally, some restraints were used including SIMU and DFIX in the final refinement. Details of the data are summarized in Table 1.

CCDC: 939840, **Zr-MC-1**; 939841, **Zr-MC-2**.

Table 1 Crystal data and structure refinement parameters for Zr-MC-1 and Zr-MC-2

Compound	Zr-MC-1	Zr-MC-2
Empirical formula	$C_{72}H_{62}Cl_2O_{21}Zr_6$	$C_{66}H_{60}Cl_2O_{23}Zr_6$
Formula weight	1 881.43	1 839.36
Temperature / K	295.01	295.01
Crystal system	Monoclinic	Monoclinic
Space group	$P2_1/m$	$C2/c$
a / nm	1.350 6(2)	2.039 4(2)
b / nm	1.604 3(3)	1.988 9(2)
c / nm	1.675 7(3)	1.789 29(18)
β / (°)	90.650(8)	105.434(5)
V / nm^3	3.630 6(10)	6.996 0(12)
Z	2	4
D_c / (g·cm^{-3})	1.721	1.746
Absorption coefficient / mm^{-1}	8.108	8.419
F(000)	1 872	3 656
Reflection collected	30 261	47 019
Independent reflection	6 627	6 912
R_{int}	0.052 7	0.046 8
Goodness-of-fit on F^2	1.066	1.042
Final R indices [$I>2\sigma(I)$][a, b]	R_1=0.070 0, wR_2=0.149 3	R_1=0.040 2, wR_2=0.095 1
R indices (all data)	R_1=0.091 0, wR_2=0.165 0	R_1=0.047 9, wR_2=0.101 1

[a] $R_1=\sum||F_o|-|F_c||/\sum|F_o|$; [b] $wR_2=\{\sum[w(F_o^2-F_c^2)^2]/\sum[w(F_o^2)^2]\}^{1/2}$

2 Results and discussion

2.1 Structure descriptions of Zr-MC-1 and Zr-MC-2

Reaction of Cp_2ZrCl_2 and linear dicarboxylate ligands (4,4′-H_2BPDC for **Zr-MC-1** and 2,6-H_2NDC for **Zr-MC-2**) in a mixed solvent system including DMF, CH_3OH and distilled water at 80 ℃ gave rise to two nanosized molecular capsules (Zr-MCs). As previously reported by Yuan et al.[16], the cationic $Cp_3Zr_3(\mu_3\text{-O})(\mu_2\text{-OH})_3$ SBUs are derived from the slow hydrolysis process of Cp_2ZrCl_2 in the existence of water (Fig.1). The carboxylate ligands in the SBUs (close to C_3 symmetry) are oriented to one face while the μ-OH species are oriented to the other, where the C_2 axes in carboxylate ligands create an angle of approximately 60°. In this connection, the substitution of the primary carboxylate in $Cp_3Zr_3(\mu_3\text{-O})(\mu_2\text{-OH})_3$ by the linear 4,4′-H_2BPDC and 2,6-H_2NDC ligands was realized in this system.

Structural analysis (Table 1) indicates that **Zr-MC-1** and **Zr-MC-2** both crystallize in the monoclinic system with corresponding $P2_1/m$ and $C2/c$ space group, respectively. Two molecular capsules

representing V_2E_3 (V =vertex and E =edge) topology could be regarded as two $Cp_3Zr_3(\mu_3\text{-}O)(\mu_2\text{-}OH)_3$ SBUs as the vertices and three associated ligands as the edges. Similar topology in Zr-MCs including the flexible sulfonate-carboxylate ligand has already been reported by Zang et al[18]. Such type of capsules with a well-known linear connection between the metal SBUs and organic species remains excellent candidate in metal-organic supercontainers. As described in Fig.2, the capsule inner (yellow column) pore sizes of the

Fig.1　Diagrammatic sketch of the formation of trinuclear $Cp_3Zr_3(\mu_3\text{-}O)(\mu_2\text{-}OH)_3$ SBUs

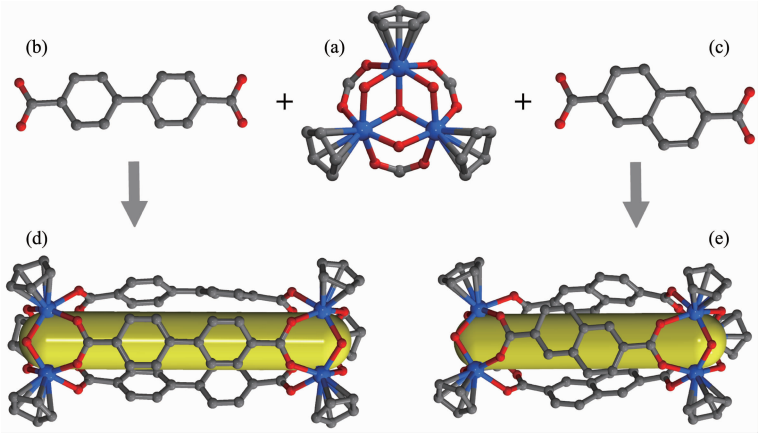

Color code: C: gray; O: red; Zr: blue. The free space in the polyhedra is filled with capsular cages. For clarity, H atoms are omitted

Fig.2　Ball-and-stick representation of $[Cp_3Zr_3(\mu_3\text{-}O)(\mu_2\text{-}OH)_3]_2$ SBUs (a), 4,4′-BPDC ligand (b), 2,6-NDC ligand (c), **Zr-MC-1** (d), and **Zr-MC-2** (e)

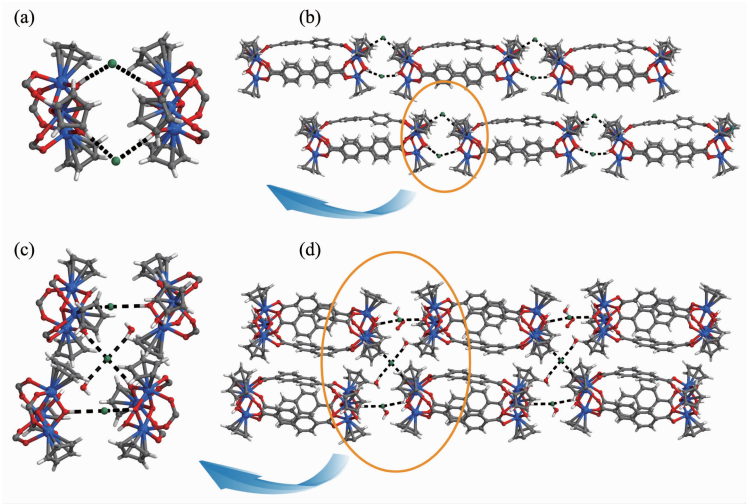

Fig.3　Hydrogen-bonding in **Zr-MC-1** (a) and 3D stacking of **Zr-MC-1** (b); Hydrogen-bonding in **Zr-MC-2** (c) and 3D stacking of **Zr-MC-2** (d)

cages are about 1.3 and 1.1 nm (the distance between two μ_3-O atoms in both zirconocene SBUs), respectively. Just as expected, this distinction is attributed to the lengths of 4,4′-H_2BPDC and 2,6-H_2NDC ligands. In both crystal structures, hydrogen bonds (O–H···Cl···H–O) among Cl^-, μ_2-OH on zirconocene and free water not only form the three-dimensional supramolecular networks of MCs but also balance the framework charge. Furthermore, selected bond distances and bond angles of **Zr-MC-1** and **Zr-MC-2** are listed in Table 2.

Table 2 Selected bond lengths (nm) and angles (°) for Zr-MC-1 and Zr-MC-2

Zr-MC-1					
Zr(1)-O(1)	0.207 1(8)	Zr(1)-O(11)	0.220 3(6)	Zr(1)-C(33)	0.252 7(11)
Zr(1)-O(6)#1	0.214 4(6)	Zr(1)-C(32)#1	0.250 6(10)	Zr(1)-C(33)#1	0.252 7(11)
Zr(1)-O(6)	0.214 4(6)	Zr(1)-C(32)	0.250 6(10)	Zr(1)-C(46)	0.250 7(16)
Zr(1)-O(11)#1	0.220 3(6)				
O(1)-Zr(1)-O(6)	73.2(2)	O(6)-Zr(1)-C(32)#1	79.7(3)	O(11)#1-Zr(1)-C(33)	112.1(4)
O(1)-Zr(1)-O(6)#1	73.2(2)	O(6)-Zr(1)-C(32)	101.8(3)	O(11)-Zr(1)-C(33)#1	112.1(4)
O(1)-Zr(1)-O(11)	79.2(2)	O(6)#1-Zr(1)-C(32)	79.7(3)	O(11)#1-Zr(1)-C(33)#1	77.9(3)
O(1)-Zr(1)-O(11)#1	79.2(2)	O(6)-Zr(1)-C(33)	130.4(3)	O(11)-Zr(1)-C(46)	81.7(3)
O(1)-Zr(1)-C(32)	152.1(3)	O(6)-Zr(1)-C(33)#1	90.7(4)	O(11)#1-Zr(1)-C(46)	81.7(3)
O(1)-Zr(1)-C(32)#1	152.1(3)	O(6)#1-Zr(1)-C(33)	90.7(4)	C(32)#1-Zr(1)-C(32)	30.7(6)
O(1)-Zr(1)-C(33)#1	153.0(3)	O(6)#1-Zr(1)-C(33)#1	130.4(3)	C(32)-Zr(1)-C(33)#1	51.3(4)
O(1)-Zr(1)-C(33)	153.0(3)	O(6)-Zr(1)-C(46)	122.2(3)	C(32)#1-Zr(1)-C(33)	51.3(4)
O(1)-Zr(1)-C(46)	154.2(5)	O(6)#1-Zr(1)-C(46)	122.2(3)	C(32)#1-Zr(1)-C(33)#1	30.8(4)
O(6)-Zr(1)-O(6)#1	92.6(3)	O(11)-Zr(1)-O(11)#1	83.7(3)	C(32)-Zr(1)-C(33)	30.8(4)
O(6)#1-Zr(1)-O(11)#1	151.7(2)	O(11)-Zr(1)-C(32)	105.5(3)	C(32)#1-Zr(1)-C(46)	51.1(5)
O(6)-Zr(1)-O(11)	151.7(2)	O(11)-Zr(1)-C(32)#1	128.4(3)	C(32)-Zr(1)-C(46)	51.1(5)
O(6)-Zr(1)-O(11)#1	85.2(2)	O(11)#1-Zr(1)-C(32)#1	105.5(3)	C(33)-Zr(1)-C(33)#1	52.2(6)
O(6)#1-Zr(1)-O(11)	85.2(2)	O(11)#1-Zr(1)-C(32)	128.4(3)	C(46)-Zr(1)-C(33)	31.5(4)
O(6)#1-Zr(1)-C(32)#1	101.8(3)	O(11)-Zr(1)-C(33)	77.9(3)	C(46)-Zr(1)-C(33)#1	31.5(4)
Zr-MC-2					
Zr(1)-O(2)	0.212 2(3)	Zr(1)-O(8)#1	0.219 6(3)	Zr(1)-C(8)	0.249 9(4)
Zr(1)-O(3)	0.213 9(3)	Zr(1)-C(6)	0.252 6(4)	Zr(1)-C(9)	0.250 0(4)
Zr(1)-O(4)	0.209 1(3)	Zr(1)-C(7)	0.251 5(4)	Zr(1)-C(10)	0.251 8(4)
Zr(1)-O(6)	0.218 4(3)				
O(2)-Zr(1)-O(3)	90.75(12)	O(4)-Zr(1)-O(2)	73.47(11)	O(8)#1-Zr(1)-C(6)	125.01(14)
O(2)-Zr(1)-O(6)	151.84(11)	O(4)-Zr(1)-O(3)	72.75(11)	O(8)#1-Zr(1)-C(7)	116.91(17)
O(2)-Zr(1)-O(8)#1	85.60(13)	O(4)-Zr(1)-O(6)	78.87(11)	O(8)#1-Zr(1)-C(8)	85.77(17)
O(2)-Zr(1)-C(6)	114.45(18)	O(4)-Zr(1)-O(8)#1	79.44(11)	O(8)#1-Zr(1)-C(9)	74.00(14)
O(2)-Zr(1)-C(7)	84.79(16)	O(4)-Zr(1)-C(6)	153.60(13)	O(8)#1-Zr(1)-C(10)	97.30(17)
O(2)-Zr(1)-C(8)	81.40(14)	O(4)-Zr(1)-C(7)	152.01(14)	C(7)-Zr(1)-C(6)	30.96(8)
O(2)-Zr(1)-C(9)	108.91(17)	O(4)-Zr(1)-C(8)	151.61(13)	C(7)-Zr(1)-C(10)	51.25(12)
O(2)-Zr(1)-C(10)	132.08(14)	O(4)-Zr(1)-C(9)	152.96(13)	C(8)-Zr(1)-C(6)	51.34(12)
O(3)-Zr(1)-O(6)	85.99(12)	O(4)-Zr(1)-C(10)	154.23(13)	C(8)-Zr(1)-C(7)	31.14(8)
O(3)-Zr(1)-O(8)#1	151.82(11)	O(6)-Zr(1)-O(8)#1	84.26(12)	C(8)-Zr(1)-C(9)	31.21(8)
O(3)-Zr(1)-C(6)	81.78(14)	O(6)-Zr(1)-C(6)	92.77(17)	C(8)-Zr(1)-C(10)	51.42(12)
O(3)-Zr(1)-C(7)	90.48(17)	O(6)-Zr(1)-C(7)	123.15(16)	C(9)-Zr(1)-C(6)	51.31(12)

Continued Table 2

O(3)-Zr(1)-C(8)	121.33(17)	O(6)-Zr(1)-C(8)	123.81(15)	C(9)-Zr(1)-C(7)	51.44(12)
O(3)-Zr(1)-C(9)	133.04(14)	O(6)-Zr(1)-C(9)	93.38(16)	C(9)-Zr(1)-C(10)	31.09(8)
O(3)-Zr(1)-C(10)	105.70(17)	O(6)-Zr(1)-C(10)	75.37(13)	C(10)-Zr(1)-C(6)	30.94(8)

Symmetry codes: #1: x, $-y+3/2$, z for **Zr-MC-1**; #1: $-x+1$, y, $-z+1/2$ for **Zr-MC-2**

2.2 Powder X-ray diffraction (PXRD) and thermogravimetric analysis (TGA)

The phase purities of **Zr-MC-1** and **Zr-MC-2** were verified by PXRD. The uniform patterns between the experimental and simulated results give evidence of pure target samples, and the crystalline structures of both MCs remained unchanged after the water treatment (Fig.4). In order to test the thermal stabilities of the two crystals, the TGA experiment was carried out between 25 and 800 ℃ under N_2 atmosphere. The weight loss below 100 ℃ indicates the loss of physically absorbed water molecules, and chloride ions and lattice water molecules were released afterwards. Finally, **Zr-MC-1** and **Zr-MC-2** lost weight drastically at ~500 ℃ (Fig.5).

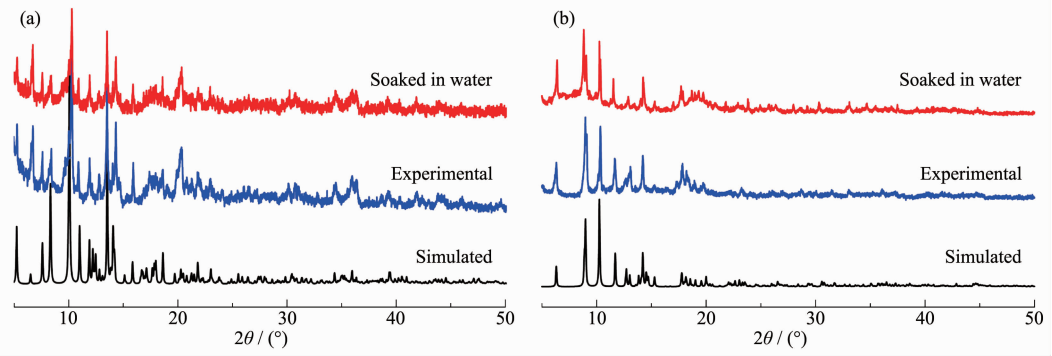

Fig.4　Experimental and simulated powder X-ray diffraction patterns for **Zr-MC-1** (a) and **Zr-MC-2** (b)

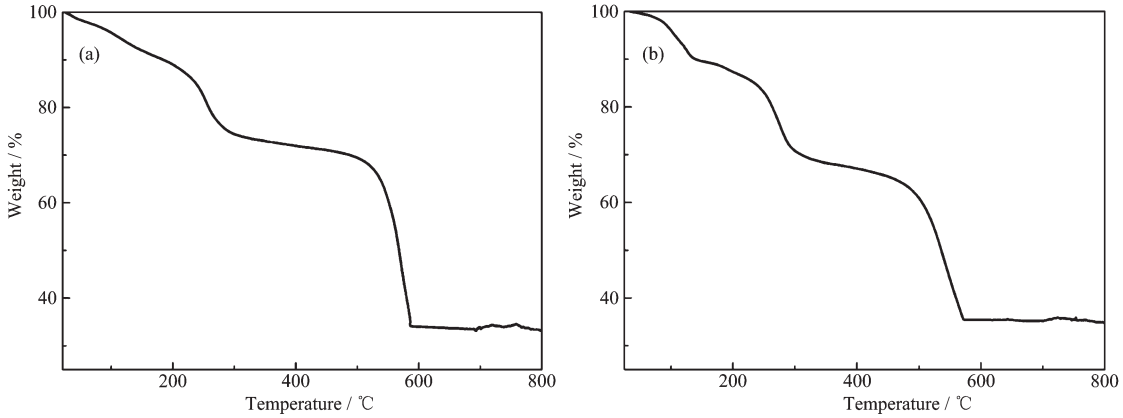

Fig.5　TG curves for **Zr-MC-1** (a) and **Zr-MC-2** (b)

2.3 Infrared spectroscopy (IR)

IR spectroscopy is an effective mean for the analysis of organic ligands and zirconocene SBUs in the crystal structures. For this purpose, IR spectra of two MCs were measured in KBr pellets. As presented in Fig.6, the absorption peaks in 400~1 200 cm^{-1} region belong to zirconium-oxygen characteristic stretching vibrations[25]. The peaks located at 3 420 cm^{-1} for **Zr-MC-1** and 3 198 cm^{-1} for **Zr-MC-2** could be assigned to the vibration of the OH group, because of the exists of μ_2-OH species and free water molecules in the crystals[26]. There was no absorption band in the region from 1 690 to 1 730 cm^{-1}, showing that 4,4′-H_2BPDC and 2,6-H_2NDC groups in **Zr-MC-1** and **Zr-MC-2** are deprotonated [26]. Furthermore, the peaks of 1 415 cm^{-1} (1 608 cm^{-1}) for **Zr-MC-1** and 1 419 cm^{-1}

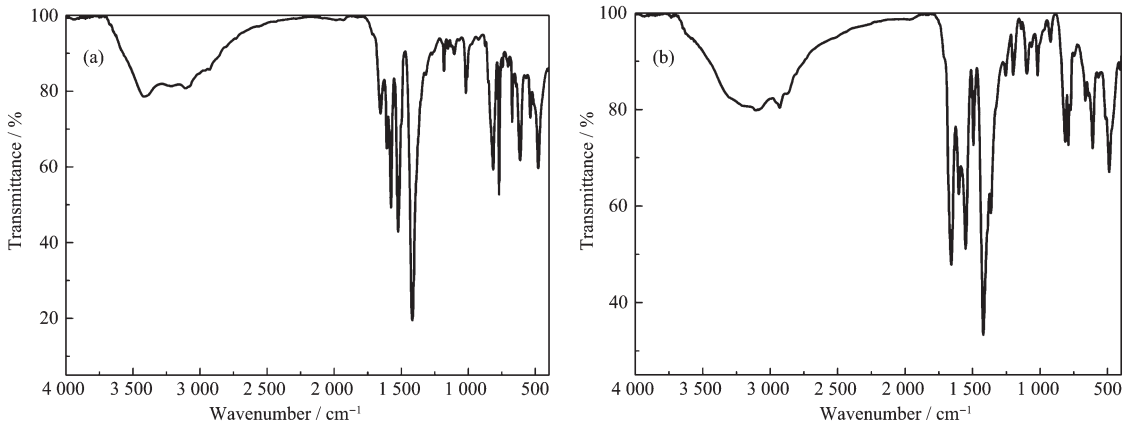

Fig.6 IR spectra for **Zr-MC-1** (a) and **Zr-MC-2** (b)

(1 599 cm^{-1}) for **Zr-MC-2** are attributed to the symmetric (asymmetric) C-O stretching vibrations[27].

2.4 N_2 adsorption measurements

In the light of capsule inner pores and pore connectivity in **Zr-MC-1** and **Zr-MC-2**, N_2 adsorption experiments were determined at 77 K. Fresh samples (150 mg) were solvent-exchanged with dichloromethane several times for 3 days, and then the soaking samples were further activated at 60 ℃ for 12 hours for next test. As shown in Fig.7a, a hysteresis loop was identified through the relative pressure P/P_0 ranging from 0.4 to 1.0 for **Zr-MC-1**. The isotherm could be assigned to the typical Ⅳ isotherm on the basis of the IUPAC classification[20]. Similar observations are also occurred for **Zr-MC-2** (Fig.7c). From Fig.7b and 7d, it may be concluded that both MCs are mesoporous

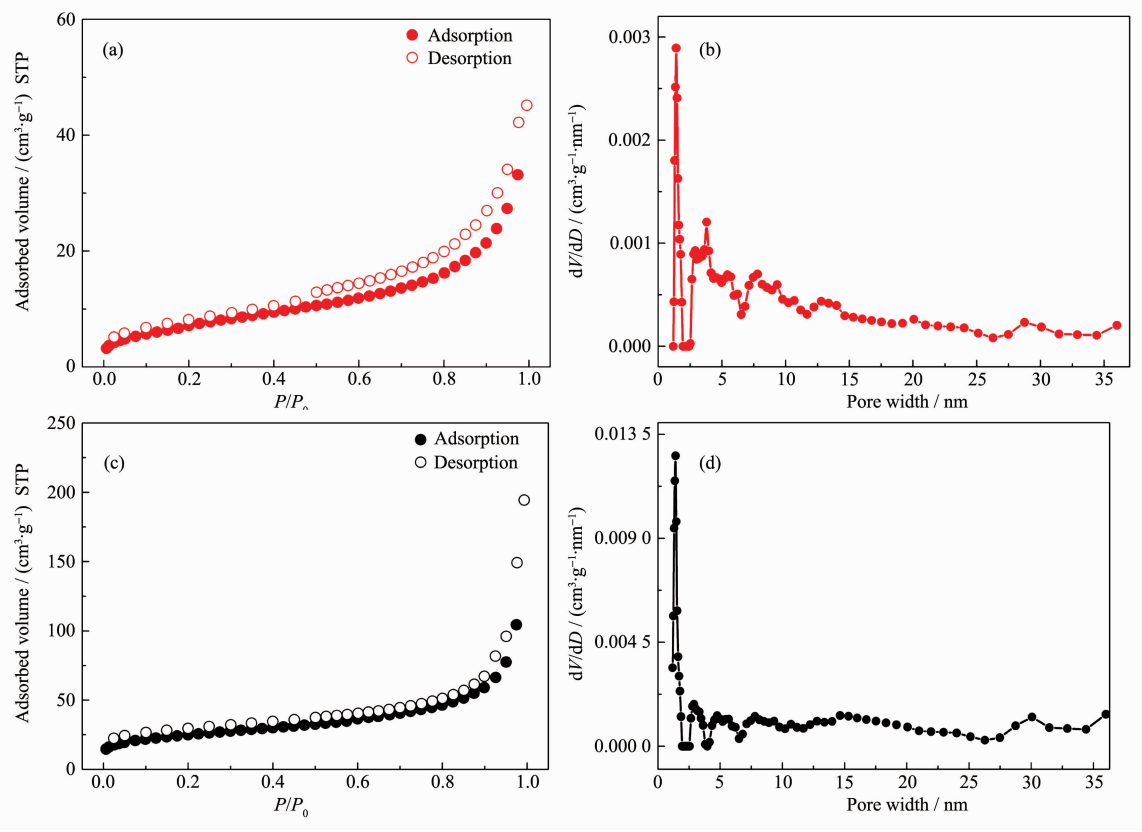

Fig.7 N_2 adsorption-desorption isotherms of **Zr-MC-1** (a) and **Zr-MC-2** (c) at 77 K; Pore size distributions of **Zr-MC-1** (b) and **Zr-MC-2** (d)

materials. The noticeable Brunauer-Emmett-Teller (BET) and Langmuir surface areas of **Zr-MC-1** were 28 and 44 $m^2 \cdot g^{-1}$, respectively. The pore volume is 0.089 4 nm^3 and the porosity is 2.5% according to the PLATON routine. Similarly, BET surface areas and Langmuir surface areas of **Zr-MC-2** are 90 and 132 $m^2 \cdot g^{-1}$, respectively. The pore volume is 0.354 nm^3 and the porosity is 5.1% based on the calculated results from the PLATON routine[20].

2.5 Luminescence property

The solid-state photoluminescence (PL) spectra of **Zr-MC-1** and **Zr-MC-2** as well as corresponding dicarboxylate ligands were investigated at room temperature. As depicted in Fig.8, on the principle of $\pi^* \rightarrow n$ transitions of the intraligands in either free ligands, 4,4′-H_2BPDC ligand (red line, Fig.8a) shows an emission at 407 nm (λ_{ex}=330 nm) while the strong emission peak of 2,6-H_2NDC ligand (red line, Fig.8b) is located at 424 nm (λ_{ex}=380 nm)[28-29]. With respect to **Zr-MC-1** (black line, Fig.8a), the emission (404 nm, λ_{ex}=330 nm) is mainly derived from 4,4′-H_2BPDC ligand. Conversely, Zr-MC-2 exhibited an apparent red-shifted emission (456 nm, λ_{ex}=380 nm) compared to 2,6-H_2NDC ligand, this phenomenon is not strange and should be assigned to ligand-to-metal charge transfer (LMCT) process. What′ s more, these observations indicate that **Zr-MC-1** and **Zr-MC-2** might be excellent candidates of deep-blue and blue-light-emitting materials, respectively.

Additionally, the luminescence decay curves of **Zr-MC-1** and **Zr-MC-2** were also measured at room temperature. As shown in Fig.9, the luminescence lifetimes of both MCs are quite different: the lifetime of **Zr-MC-1** (λ_{ex}=330 nm) and **Zr-MC-2** (λ_{ex}=380 nm) are 1.48 and 17.02 ns, respectively. This fact may be attributed to that the rigidity of 2,6-H_2NDC ligand is stronger in contrast to 4,4′-H_2BPDC ligand, thus the much weaker vibrations in **Zr-MC-2** effectively reduce the loss of energy by radiationless decay[30].

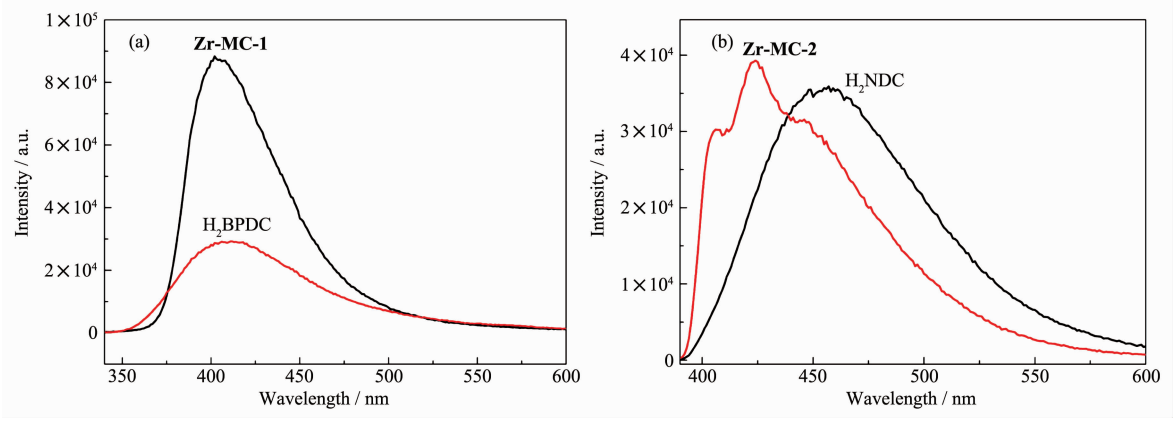

Fig.8 (a) Emission spectra of 4,4′-H_2BPDC and **Zr-MC-1**, (b) Emission spectra of 2,6-H_2NDC and **Zr-MC-2**

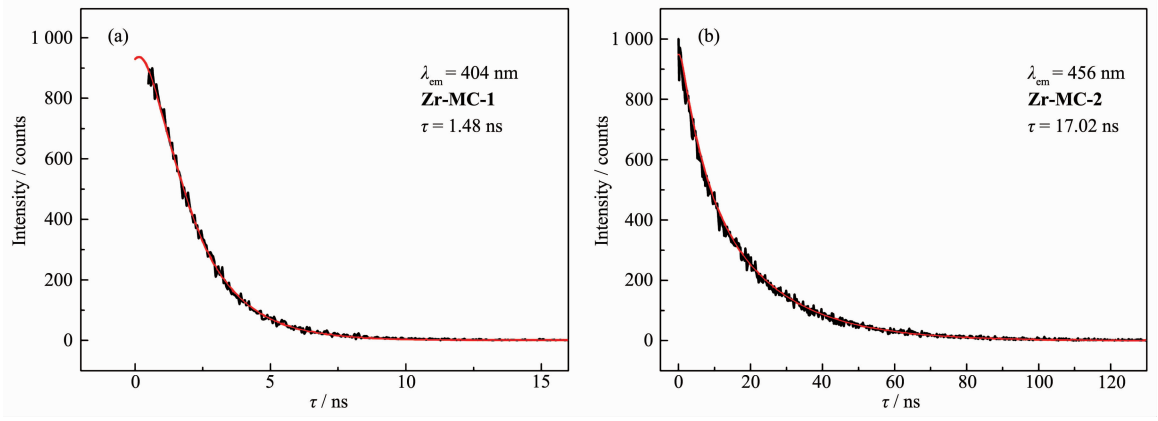

Fig.9 Solid state fluorescence decay curves of **Zr-MC-1** (a) and **Zr-MC-2** (b)

3 Conclusions

In summary, two new nanosized Zr-based MCs constructed from trinuclear $Cp_3Zr_3(\mu_3\text{-}O)(\mu_2\text{-}OH)_3$ SBUs and linear dicarboxylate ligands have been successfully synthesized under solvothermal conditions. Two crystals were fully characterized by multiple analysis techniques and their photoluminescent properties indicate that both complexes might be excellent candidates of blue-light-emitting diode devices. The obtained conclusions could inspire further achievements in connection with the exploration of diverse coordination zirconocene molecular capsules with amazing architectures and desired functionalities to be realized.

Acknowledgements: This work was financially supported by the NSFC of China (Grants No.21801038, 21471027, 21671034), the Science and Technology Research Foundation of the Thirteenth Five Years of Jilin Educational Committee (Grant No.JJKH20190271KJ), the China Postdoctoral Science Foundation funded project (Grants No.2018M630312, 2019T120227), and the Fundamental Research Funds for the Central Universities (Grant No.2412018QD003).

References:

[1] Tranchemontagne D J, Ni Z, O′Keeffe M, et al. *Angew. Chem. Int. Ed.*, **2008**,**47**(28):5136-5147

[2] Wu K, Li K, Hou Y J, et al. *Nat. Commun.*, **2016**,**7**:10487

[3] Li J R, Zhou H C. *Nat. Chem.*, **2010**,**2**(10):893-898

[4] Kang Y H, Liu X D, Yan N, et al. *J. Am. Chem. Soc.*, **2016**, **138**(19):6099-6102

[5] Li J R, Zhou H C. *Angew. Chem. Int. Ed.*, **2009**,**48**(45):8465-8468

[6] Lorzing G R, Trump B A, Brown C M, et al. *Chem Mater.*, **2017**,**29**(20):8583-8587

[7] Zhang Y T, Wang X L, Li S B, et al. *Chem. Commun.*, **2016**, **52**(62):9632-9635

[8] Zhang Y T, Li S B, Wang X L, et al. *Dalton Trans.*, **2016**,**45** (38):14898-14901

[9] Zhang Y T, Gan H M, Qin C, et al. *J. Am. Chem. Soc.*, **2018**, **140**:17365-17368

[10]Kim J, Chua V, Fiete G A, et al. *Nat. Commun.*, **2018**,**9** (4941):1-6

[11]Zhao D, Tan S W, Yuan D Q, et al. *Adv. Mater.*, **2011**,**23** (1):90-93

[12]Ahmad N, Younus H A, Chughtai A H, et al. *Chem. Soc. Rev.*, **2015**,**44**(1):9-25

[13]Fang Y, Xiao Z F, Kirchon A, et al. *Chem. Sci.*, **2019**,**10**: 3529-3534

[14]Meng W J, Breiner B, Rissanen K, et al. *Angew. Chem. Int. Ed.*, **2011**,**50**(15):3479-3483

[15]Liu G L, Yuan D Y, Wang J, et al. *J. Am. Chem. Soc.*, **2018**, **140**(20):6231-6234

[16]Liu G L, Ju Z F, Yuan D Q, et al. *Inorg. Chem.*, **2013**,**52** (24):13815-13817

[17]Jiao J J, Tan C X, Li Z J, et al. *J. Am. Chem. Soc.*, **2018**, **140**(6):2251-2259

[18]Xing W H, Li H Y, Dong X Y, et al. *J. Mater. Chem. A*, **2018**,**6**(17):7724-7730

[19]Lee S, Lee J H, Kim J C, et al. *ACS Appl. Mater. Interfaces*, **2018**,**10**(10):8685-8691

[20]Ju Z F, Liu G L, Chen Y S, et al. *Chem. Eur. J.*, **2017**,**23**: 4774-4777

[21]Nam D, Huh J, Lee J, et al. *Chem. Sci.*, **2017**,**8**(11):7765-7771

[22]Liu G L, Zeller M, Su K Z, et al. *Chem. Eur. J.*, **2016**,**22**: 17345-17350

[23]Sun M, Wang Q Q, Qin C, et al. *Chem. Eur. J.*, **2019**,**25**: 2824-2830

[24]Sheldrick G M. *SHELXL*-2014, *Programs for Crystal Structure Refinement*, University of Göttingen, Germany, 2014.

[25]CHEN Shou-Gan(陈守刚), YU Mei-Yan(于美燕), HU Bao-Ge(胡保革), et al. *Journal of the Chinese Ceramic Society* (硅酸盐学报), **2017**,**35**(1):46-51

[26]CHENG Mei-Ling(程美令), YANG Bing-Xin(杨冰心), TANG Li-Zhi-Peng(唐李志鹏), et al. *Chinese J. Inorg. Chem.*(无机化学学报), **2019**,**35**(4):687-694

[27]Peh S B, Cheng Y D, Zhang J, et al. *Dalton Trans.*, **2019**, **48**:7069-7073

[28]Wang X L, Qin C, Wang E B, et al. *Inorg. Chem.*, **2004**,**43**: 1850-1856

[29]Yang J, Yue Q, Li G D, et al. *Inorg. Chem.*, **2006**,**45**:2857-2865

[30]Du D Y, Qin J S, Sun C X, et al. *J. Mater. Chem.*, **2012**,**22**: 19673-19678